

UC Irvine

UC Irvine Previously Published Works

Title

A Recent Shift in the Monsoon Centers Associated with the Tropospheric Biennial Oscillation

Permalink

<https://escholarship.org/uc/item/535441bs>

Journal

Journal of Climate, 31(1)

ISSN

0894-8755

Authors

Wang, Lei
Yu, Jin-Yi

Publication Date

2018

DOI

10.1175/jcli-d-17-0349.1

Peer reviewed



AMERICAN METEOROLOGICAL SOCIETY

Journal of Climate

EARLY ONLINE RELEASE

This is a preliminary PDF of the author-produced manuscript that has been peer-reviewed and accepted for publication. Since it is being posted so soon after acceptance, it has not yet been copyedited, formatted, or processed by AMS Publications. This preliminary version of the manuscript may be downloaded, distributed, and cited, but please be aware that there will be visual differences and possibly some content differences between this version and the final published version.

The DOI for this manuscript is doi: 10.1175/JCLI-D-17-0349.1

The final published version of this manuscript will replace the preliminary version at the above DOI once it is available.

If you would like to cite this EOR in a separate work, please use the following full citation:

Wang, L., and J. Yu, 2017: A Recent Shift in the Monsoon Centers associated with the Tropospheric Biennial Oscillation. *J. Climate*. doi:10.1175/JCLI-D-17-0349.1, in press.

© 2017 American Meteorological Society



1
2
3 **A Recent Shift in the Monsoon Centers associated with the**
4 **Tropospheric Biennial Oscillation**
5
6
7

8 Lei Wang^{1,2} and Jin-Yi Yu²
9

10 ¹Guangdong Province Key Laboratory for Coastal Ocean Variation and Disaster
11 Prediction, College of Ocean and Meteorology, Guangdong Ocean University,
12 Zhanjiang 524088, China (leiwangocean@yahoo.com)

13 ²Department of Earth System Science, University of California, Irvine, California
14 92697, USA (jyyu@uci.edu)

15
16
17
18 Revised, *Journal of Climate*

19
20 September, 2017
21
22
23
24
25
26
27
28
29
30

Abstract

31

32

33 The tropospheric biennial oscillation (TBO) is conventionally considered to involve
34 transitions between the Indian and Australian summer monsoons and the interactions
35 between these two monsoons and the underlying Indo-Pacific Oceans. Here we show
36 that, since the early 1990s, the TBO has evolved to mainly involve the transitions
37 between the western North Pacific (WNP) and Australian monsoons. In this
38 framework, the WNP monsoon replaces the Indian monsoon as the active northern
39 hemisphere TBO monsoon center during recent decades. This change is found to be
40 caused by stronger Pacific-Atlantic coupling and an increased influence of the tropical
41 Atlantic Ocean on the Indian and WNP monsoons. The increased Atlantic Ocean
42 influence damps the Pacific Ocean influence on the Indian summer monsoon (leading
43 to a decrease in its variability) but amplifies the Pacific Ocean influence on the WNP
44 summer monsoon (leading to an increase in its variability). These results suggest that
45 the Pacific-Atlantic interactions have become more important to the TBO dynamics
46 during recent decades.

47

48

49

50

51 **1. Introduction**

52 The tropical Indo-Pacific sector encompasses two of the most active monsoons
53 in our climate system: the Indian monsoon located in the northern part of the sector
54 and the Australian monsoon in the southern part. The tropospheric biennial oscillation
55 (TBO) is a major variation of the Indian-Australian monsoon system, with years of
56 strong summer rainfall more likely to be followed by years of weak rainfall and vice
57 versa (*Meehl 1987, 1994, 1997; Meehl and Arblaster 2002a*). Previous studies have
58 already revealed that the biennial variations in the Indian summer monsoon and the
59 Australian summer monsoon tend to be related to each other (e.g., *Matsumoto 1992;*
60 *Yu et al. 2003; Hung et al. 2004*). This relation is manifested as an in-phase transition
61 from the Indian summer monsoon to the Australian summer monsoon (i.e., a strong
62 Indian monsoon in boreal summer is followed by a strong Australian summer
63 monsoon in the following austral summer and vice versa) and an out-of-phase
64 transition from the Australian summer monsoon back to the Indian summer monsoon
65 in the next year (i.e., a strong Australian summer monsoon is followed by a weak
66 Indian summer monsoon and vice versa). These in-phase and out-of-phase transitions
67 between the Indian and Australian monsoons are two key features of the TBO (*Yu et*
68 *al. 2003*) and are referred to as the biennial monsoon transitions in this study.

69 Much effort has been expended trying to understand TBO dynamics and the
70 associated monsoon transitions, resulting in substantial advances in our understanding
71 of this important climate phenomenon. It is generally agreed that the interactions
72 between the monsoons and the tropical Indian and Pacific Oceans play a central role
73 in the TBO dynamics (e.g., *Nicholls 1978, 1979, 1984; Meehl 1987, 1993; Clarke et*
74 *al. 1998; Chang and Li 2000; Meehl et al. 2003; Li et al. 2006; Zheng et al. 2008*).
75 This is based on the observational finding that the biennial variations in monsoon

76 rainfall are associated with significant variations at similar timescales in the sea
77 surface temperatures (SSTs) of the tropical Indian and Pacific Oceans (*Rasmusson*
78 *and Carpenter 1983; Meehl 1987; Kiladis and van Loon 1988; Ropelewski et al.*
79 *1992; Lau and Yang 1996; Meehl and Arblaster 2002b; Yu et al. 2003*). The
80 associated SST anomalies are characterized by an El Niño-Southern Oscillation
81 (ENSO)-type pattern in the Pacific Ocean and a basin-scale warming or cooling in the
82 Indian Ocean, or an east-west dipole along the equatorial Indian Ocean that is known
83 as the Indian Ocean Dipole (IOD) or Indian Ocean Zonal Mode (*Webster et al. 1999;*
84 *Saji et al. 1999*).

85 *Meehl (1993)* proposed that the in-phase monsoon transition is produced by
86 local monsoon-ocean interactions in the Indian and western Pacific Oceans associated
87 with the southeastward migration of convection during the annual cycle. The Indian
88 summer monsoon winds force SST anomalies around Australian (via ocean
89 upwelling/downwelling and mixing) that persist into the following boreal winter and
90 affect the strength of the Australian summer monsoon. For the out-of-phase monsoon
91 transition, the Australian summer monsoon wind forces oceanic waves in the western
92 Pacific Ocean that propagate into the eastern Pacific to influence SST anomalies
93 there. These SST anomalies later influence the strength of the Indian summer
94 monsoon through the large-scale east-west atmospheric circulation. In this theory, it is
95 the interaction between the monsoons and the eastern Pacific Ocean that provides the
96 phase-reversal mechanism for the TBO. *Chang and Li (2000)* also related the
97 monsoon-ocean interactions to the TBO but did not emphasize the interaction between
98 the Australian monsoon and the eastern Pacific. Instead, they suggested that a strong
99 Australian summer monsoon enhances the Walker circulation over the Indian Ocean
100 and produces strong westerly anomalies in the central Indian Ocean. These wind

101 anomalies help to cool Indian Ocean SSTs through processes such as wind and latent
102 and sensible heat fluxes. The cold SST anomalies persist into the following boreal
103 summer to produce a weak Indian summer monsoon by reducing the moisture
104 available. Regardless of the differences, these theories emphasize the interactions
105 between Indian-Australian summer monsoons and the Indo-Pacific Oceans to explain
106 how the TBO and the monsoon transitions can be produced.

107 However, in addition to the Indian monsoon, there are other sub-components
108 in the Asian monsoon system including the East Asian monsoon and the western
109 North Pacific (WNP) monsoon (e.g., *Wang et al. 2001*). *Lee et al. (2014)* examined
110 the interdecadal changes in global monsoon variability and noticed that the
111 interannual variability of the WNP monsoon has increased and become a dominant
112 component of the Asian summer monsoon variability after 1993. They found the WNP
113 summer monsoon variability after 1993 tends to be related to the central-Pacific (CP)
114 type El Nino-Southern Oscillation (ENSO) events (*Yu and Kao 2007; Kao and Yu*
115 *2009*), which have also occurred more frequently since the early 1990s (*Yu et al. 2012;*
116 *Yu et al. 2015*). These recent changes in ENSO and the monsoons may have modified
117 the characteristics of the TBO in recent decades, particularly the associated biennial
118 monsoon transitions. Furthermore, recent studies on the early-1990s change in ENSO
119 types have suggested that this change may be related to the increased influences of the
120 Atlantic Ocean on the Pacific climate (*Yu et al. 2015; Lyu et al. 2017; Wang et al.*
121 *2017*), which is associated with a change of the Atlantic Multi-decadal Oscillation
122 (AMO; *Schlesinger and Ramankutty 1994; Kerr 2000*) from a negative to a positive
123 phase around that time. There is also increasing evidence to support a significant
124 influence of the tropical Atlantic SST on the variability of the Indian summer
125 monsoon (*Kucharski et al. 2007, 2008; Cash et al. 2013*) and Pacific climate

126 variability (*Rodríguez-Fonseca et al. 2009; Keenlyside et al. 2013; Hong et al. 2014;*
127 *Yu et al. 2015; Li et al. 2016*). Therefore, it is possible that the Atlantic Ocean may
128 have become important to the TBO dynamics. It is necessary to know how these
129 Atlantic influences may have modified the biennial monsoon transitions of the TBO
130 in recent decades.

131 In this study, we perform statistical analyses using observations and reanalysis
132 products to examine the decadal changes in the TBO and its biennial monsoon
133 transitions since 1948. This paper is organized as follows. The data used and the
134 analysis procedures are described in section 2. The changes in the biennial monsoon
135 transitions in the TBO since the early 1990s are presented in Section 3. Section 4
136 illustrates the influences of tropical Atlantic SST anomalies on the recent change in
137 the biennial monsoon transitions. Conclusions and discussion are given in the final
138 section (Section 5).

139

140 **2. Data and methods**

141 The SST data used here are the monthly extended reconstructed SST (ERSST)
142 analyses (*Smith et al. 2008*). The atmospheric fields are from the National Centers for
143 Environmental Prediction-National Center for Atmospheric Research (NCEP-NCAR)
144 monthly reanalysis (*Kalnay et al. 1996*) that begin in 1948. The monthly rainfall data
145 used is NOAA's Precipitation Reconstruction (PREC) (*Chen et al. 2002*), which also
146 begins in 1948 and was obtained from <http://www.esrl.noaa.gov/psd/>.

147 The following dynamic monsoon indices are used in the analysis: (1) the WNP
148 monsoon index is defined, following *Wang and Fan (1999)*, as the difference in
149 850-hPa zonal winds between a southern region (5° – 15° N, 100° – 130° E) and a
150 northern region (20° – 30° N, 110° – 140° E); (2) the Indian summer monsoon index is
151 defined as the difference in the 850-hPa zonal winds between a southern region

152 (5°–15°N, 40°–80°E) and a northern region (20°–30°N, 70°–90°E) (*Wang et al.* 2001);
153 (3) the Australian monsoon index is defined as the 850-hPa zonal wind averaged over
154 the area (5°S–15°S, 110°E–130°E), following *Kajikawa et al.* (2000). These dynamic
155 monsoon indices based on 850-hPa winds have been shown to be consistent with
156 monsoon rainfall variability (*Wang et al.* 2001; *Kajikawa et al.* 2000). Following
157 *Kwon et al.* (2005), an East Asian (EA) summer rainfall index is defined as the JJA
158 precipitation anomaly averaged over the area (30°N–50°N, 115°E–150°E).

159 The Niño3.4 index is used to represent ENSO intensity and is defined as the
160 SST anomalies averaged over (5°S–5°N, 170°W–120°W). The Indian Ocean Dipole
161 Mode Index (DMI) is defined as the difference between SST anomalies in the western
162 (50°E to 70°E and 10°S to 10°N) and eastern (90°E to 110°E and 10°S to 0°S)
163 equatorial Indian Ocean (*Saji et al.* 1999). Following *Kucharski et al.* (2008), a
164 tropical South Atlantic SST index is defined as the SST anomalies averaged over
165 (20°S–0°, 30°W–10°E). Following *Hong et al.* (2014), a tropical North Atlantic SST
166 index is defined as the SST anomalies averaged over (0°–20°N, 80°W–25°E).

167 Anomalies are calculated by removing long-term trend first and then the mean
168 seasonal cycle for the period 1971–2000. The interannual variability was obtained by
169 applying a 7-yr high-pass filter to the anomalies. The intensity of the interannual
170 variability during a period is measured by the standard deviation of the interannual
171 time series during that period.

172 We classified each year during the analysis period to be a strong, weak, or
173 normal monsoon year based on whether the anomalies in the summer monsoon index
174 during that year are, respectively, above, below, or close to a threshold value.
175 Following *Wu and Kirtman* (2004), the 0.43 standard deviation was used as the
176 threshold value to ensure that the three categories (i.e., strong, weak and normal

177 monsoon years) have nearly equal numbers of years. We have also repeated the
178 classification using three other threshold values (i.e., 0.40, 0.45, and 0.50 standard
179 deviations) and found similar results. Thus, the results reported in this study are not
180 particularly sensitive to the threshold value used in the classification. Considering that
181 the biennial monsoon transitions are comprised of both in-phase and out-of-phase
182 transitions between monsoons, we then selected the in-phase and out-of-phase
183 monsoon transition years for composite analysis. An “in-phase” transition case is
184 identified if a strong (weak) summer monsoon in one hemisphere (such as the Indian
185 and WNP monsoon in the northern hemisphere or the Australian monsoon in the
186 southern hemisphere) is followed by a strong (weak) summer monsoon in the other
187 hemisphere. Similarly, an “out-of-phase” transition case is identified if a strong (weak)
188 summer monsoon in one hemisphere is followed by a weak (strong) summer monsoon
189 in the other hemisphere. For the sake of comparison in the composite analysis, if a
190 transition involves a strong Australian summer monsoon, we refer to it as a “positive”
191 in-phase or “positive” out-of-phase transition case. If the transition involves weak
192 Australian summer monsoon, that transition case is referred to as a “negative”
193 in-phase or “negative” out-of-phase transition case. The composites for the in-phase
194 transition were then constructed as the means of the “positive” in-phase transition
195 cases minus the means of the “negative” in-phase transition cases. Similarly, the
196 composites for the out-of-phase transitions were constructed as the means of the
197 “positive” out-of-phase transition cases minus the means of the “negative”
198 out-of-phase transition cases. These composites are designed to reveal the
199 atmospheric and oceanic conditions involved in the transition from a strong or weak
200 Indian/WNP summer monsoon to a strong Australian summer monsoon or from a
201 strong Australian summer monsoon back to a strong or weak Indian/WNP summer

202 monsoon.

203 The analysis methods used in this study include correlation and composite
204 analyses. We determine the statistical significance levels based on the two-tailed P
205 values using a Student's t -test.

206

207 **3. Decadal Changes in the biennial monsoon transitions of the TBO**

208 To elucidate possible decadal changes in the biennial monsoon transitions, we
209 first performed a 21-year sliding correlation analysis between the Indian monsoon
210 index during boreal summer (June-July-August; JJA) and the Australian monsoon
211 index during the following austral summer (December-January-February; DJF) for the
212 period 1948–2016 (Fig.1a). As expected, the correlation coefficients are positive
213 throughout the analysis period, which indicates that in-phase transitions from a strong
214 (weak) Indian summer monsoon to a strong (weak) Australian summer monsoon
215 dominate the time series. However, these in-phase transitions are statistically
216 significant at the 95% confidence level only during the early-1960s to the early-1980s,
217 having weakened remarkably afterward. A similar sliding analysis between the DJF
218 Australian monsoon index and the subsequent JJA Indian monsoon index shows
219 negative correlation coefficients throughout the analysis period (Fig.1a), which
220 indicates the expected out-of-phase transition from the Australian summer monsoon to
221 the following Indian summer monsoon. The negative correlations are statistically
222 significant at the 90% or 95% confidence levels during the early-1960s to the
223 early-1990s, becoming insignificant after the early-1990s. This analysis indicates that
224 the biennial monsoon transitions between the Indian and Australian monsoons were
225 strong during 1960s-1980s but have weakened in recent two decades.

226 We then performed the same 21-year sliding correlation analyses between the

227 boreal summer WNP monsoon and the austral summer Australian monsoon to
228 examine the decadal changes in their relationships. The analysis results (Fig.1b) show
229 two main differences from the relationships found between Indian and Australian
230 summer monsoons. First, the transition from the WNP summer monsoon to the
231 following Australian summer monsoon is out-of-phase (i.e., negative values in their
232 correlation coefficients) while the transition from the Australian summer monsoon to
233 the subsequent WNP summer monsoon is in-phase (i.e., positive correlation
234 coefficients). These monsoon transitions are exactly the opposite of the transitions
235 between the Indian and Australian summer monsoons. This is related to the fact that
236 the interannual variations of the WNP summer monsoon tend to be out of phase with
237 the variations of Indian summer monsoon, which has been documented by *Gu et al.*
238 (2010). They attributed this phenomenon to the different relationships between these
239 two monsoons and El Niño. During the summer of a developing El Niño, the
240 anomalously warm eastern Pacific tends to induce cyclonic wind shear over the WNP
241 that strengthens the WNP monsoon but suppresses convection over the Indian
242 monsoon region. During the subsequent summer as El Niño decays, a weak WNP
243 monsoon tends to occur due to the persistence of a local anomalous anticyclone,
244 whereas a strong Indian monsoon tends to occur due to the ENSO-induced basin-wide
245 Indian Ocean warming. The other main feature to note in Fig. 1b is that the
246 correlations between the WNP and Australian summer monsoons become stronger
247 after the early 1990s, which is the period when the correlations between Indian and
248 Australian summer monsoons weaken (see Fig.1a). These sliding correlation analyses
249 suggest that the WNP monsoon has replaced the Indian monsoon in the monsoon
250 biennial transitions associated with the TBO after the early 1990s.

251 To quantitatively assess the strength of the biennial monsoon transitions, we

252 define a biennial transition index (BTI) as follows:

$$253 \quad \text{BTI} = (-1) \times \text{Cor1} \times \text{Cor2}. \quad (1)$$

254 Here, Cor1 is the 21-year sliding correlation coefficient between the JJA Indian or
255 WNP monsoon index and the subsequent DJF Australian monsoon index, while Cor2
256 is the sliding correlation coefficient between the DJF Australian monsoon index and
257 the subsequent JJA Indian or WNP monsoon index. The factor -1 is included in Eq. (1)
258 to reflect the fact that the biennial monsoon transitions are the combination of an
259 in-phase transition (i.e., a positive correlation coefficient) and an out-of-phase
260 transition (i.e., a negative correlation coefficient). Thus, the larger the BTI value the
261 stronger the biennial transitions between the two monsoons. Fig. 1c shows the BTI
262 values calculated from the sliding correlations between the Indian/WNP summer
263 monsoons and the Australian summer monsoon. The most obvious feature in the
264 figure is that the biennial transitions were stronger between the Indian and Australian
265 summer monsoons before the early 1990s but stronger between the WNP and
266 Australian summer monsoons afterward. We also use a regime shift detection method
267 developed by *Rodionov* (2004) to confirm that the shift really occurs during the early
268 1990s. This detection method uses a regime shift index (RSI) to objectively determine
269 the time when a time series undergoes a regime shift. Previous studies have also found
270 an early-1990s shift in the WNP monsoon (e.g., *Kwon et al. 2005; Lee et al. 2014*)
271 and the WNP subtropical high (e.g., *Sui et al. 2007; Paek et al. 2016*).

272 Since the EA monsoon is another important sub-component of the Asian
273 monsoon system, we also examined the biennial relationship between the JJA EA
274 monsoon index and the Australian monsoon index. We find the correlation coefficient
275 is weak and mostly insignificant throughout the analysis period (not shown). The BTI
276 values calculated for the EA-Australian monsoon transitions were much smaller than

277 those calculated for the Indian-Australian and WNP-Australian monsoon transitions
278 (not shown). These results suggest that there were no significant biennial monsoon
279 transitions between the EA and Australian monsoons during the analysis period. This
280 may be due to the fact that the EA monsoon is located at higher latitudes than the
281 other sub-components of the Asian monsoon system and receives more extratropical
282 influences (such as those associated with mid-latitude jet stream variations) than the
283 other monsoon components.

284 According to these results, the TBO has evolved from mainly involving
285 biennial monsoon transitions between the Indian and Australian monsoons to mainly
286 involving biennial monsoon transitions between the WNP and Australian monsoons
287 since the early 1990s. Since the early 1990s, the relations between the biennial
288 tendencies in the Indian monsoon and the Australian monsoon weakened remarkably;
289 on the contrary, the relations between biennial tendencies in the WNP monsoon and
290 the Australian monsoon were greatly enhanced. To further demonstrate this change,
291 we show in Fig.2a wavelet analysis of the indices of the WNP, Indian, and Australian
292 summer monsoons. The wavelet power spectrum in Fig.2a shows that the
293 quasi-biennial (QB) band (e.g., 2-3 years) of the WNP monsoon variability
294 significantly increased after the early 1990s, which is consistent with the observed
295 fact that the leading periodicities of the summer western Pacific subtropical high also
296 shifted from the low-frequency (LF) band (e.g., 3-7 years) to the QB band in the early
297 1990s (*Sui et al. 2007; Paek et al. 2016*). However, the QB band of the Indian
298 monsoon variability weakened substantially after the 1980s (Fig.2b). For the
299 Australian monsoon, significant power in the QB band is found during nearly the
300 entire analysis period (Fig.2c). No significant changes before and after the early 1990s
301 are found for the QB band of the Australian monsoon, although the LF band of the

302 Australian monsoon was found to be suppressed greatly after the early 1990s.

303

304 **4. Influences of Atlantic SSTs on the recent TBO changes**

305 Why are different biennial monsoon transitions observed in the TBO before
306 and after the early 1990s? The biennial monsoon transitions before and after the early
307 1990s are likely to be accompanied by different SST anomalies, whose interactions
308 with the monsoons should be considered to explain the TBO changes (e.g., *Meehl*
309 *1987, 1993; Clarke et al. 1998; Chang and Li 2000; Meehl et al. 2003; Li et al. 2006*).

310 To identify the possible differences in SST anomalies involved in the biennial
311 monsoon transitions, we composited SST anomalies for the biennial transitions
312 between the Indian and Australian summer monsoons for the period before the
313 early-1990s (1967–1987, which is referred to as P1 hereafter) and between the WNP
314 and Australian summer monsoons in a period after the early-1990s (1994–2014,
315 which is referred to as P2 hereafter). These two periods correspond, respectively, to
316 the 21-year periods in Fig. 1c that produce the maximum BTI values for the
317 Indian-Australian monsoon transitions (centered around 1977) and the
318 WNP-Australian monsoon transitions (centered around 2004). During P1, the BTI
319 value for the Indian-Australian monsoon transitions is 0.347 but is only -0.062 for the
320 WNP-Australian monsoon transitions. In contrast, the BTI value during P2 is only
321 0.073 for the Indian-Australian monsoon transitions but 0.483 for the
322 WNP-Australian monsoon transitions. The correlation coefficients (Table 1) confirm
323 that the in-phase and out-of-phase transitions are both strong and significant between
324 the Indian and Australian monsoons during P1 and between the WNP and Australian
325 monsoons during P2. During P1, nine cases were selected for the in-phase transition
326 from the Indian to Australian summer monsoons (i.e., the I-to-A transition) and eight

327 cases were selected for the out-of-phase transition from the Australian to Indian
328 summer monsoons (i.e., the A-to-I transition). During P2, eleven cases were selected
329 for the out-of-phase transition from the WNP to Australian summer monsoons (i.e.,
330 the W-to-A transition) and eight cases were selected for the in-phase transition from
331 the Australian to WNP summer monsoons (i.e., the A-to-W transition). The cases
332 selected for the composite are listed in Table 2.

333 As mentioned previously, the biennial monsoon transitions during P1 mainly
334 consist of an in-phase I-to-A transition and an out-of-phase A-to-I transition. During
335 the I-to-A transitions (Fig. 3a-d), significant SST anomalies in the composite are
336 located mostly in the Pacific and Indian Oceans but not in the Atlantic Ocean. The
337 anomalies are characterized by a developing La Niña event, with the cold anomalies
338 emerging in the central-to-eastern Pacific during boreal spring, spreading westward
339 during boreal summer and autumn, and peaking in the central Pacific during austral
340 summer. In the Indian Ocean, the composite SST anomalies resemble the typical
341 Indian Ocean response to a La Niña event: a negative-phase IOD appears during
342 boreal summer and autumn (September-October-November; SON) that later evolves
343 into a basin-wide cooling in boreal winter (i.e., austral summer). These composite
344 anomalies are consistent with those found in previous studies suggesting that the TBO
345 is accompanied by El Niño/La Niña-like anomalies in the Pacific and the IOD and
346 basin-wide warming/cooling in the Indian Ocean (*Loschnigg et al. 2003; Meehl et al.*
347 *2003*). A developing La Niña is known to be capable of strengthening the Walker
348 circulation to intensify the Indian monsoon during JJA and the Australian monsoon in
349 DJF (e.g., *Chang and Li 2000; Yu et al. 2003; Gu et al. 2010*). Therefore, the in-phase
350 I-to-A transition can be maintained by the developing La Niña. The cold anomalies in
351 the Indian Ocean may also contribute to the strong Australian summer monsoon (e.g.,

352 *Taschetto et al. 2011*). The composites in atmospheric fields reveal a strong summer
353 Indian monsoon during this transition phase that is characterized by an anomalous
354 low-level cyclonic circulation (Fig.3b) and enhanced rainfall (Fig.4b) around the
355 Indian Peninsula together with anomalous descending motion (represented by
356 negative values of anomalous 850-hPa velocity potential) over the eastern Pacific and
357 anomalous ascending over the Indian monsoon region (Fig.4b).

358 As for the out-of-phase A-to-I transitions during P1 (Figs.5a-d), the composite
359 SST anomalies are most prominent in the Pacific Ocean. The anomalies are
360 characterized by a phase reversal from a decaying La Niña in DJF to an El Niño in
361 JJA that continues to develop thereafter. The decaying La Niña in DJF supports a
362 strong Australian summer monsoon, whereas the developing El Niño in JJA results in
363 a weak Indian summer monsoon. Therefore, the out-of-phase A-to-I transition can be
364 explained reasonably by this SST evolution pattern. Cold SST anomalies in the Indian
365 Ocean are large only during DJF when they may strengthen the Australian summer
366 monsoon through a Gill-type atmospheric response and by inducing anomalous
367 ascending motions over Australia (*Taschetto et al. 2011; Cai and van Rensch 2013*).
368 The composited atmospheric fields are also characterized by a weakened summer
369 Indian monsoon, with an anomalous low-level anti-cyclonic circulation (Fig.5c),
370 suppressed rainfall (Fig.6c), and anomalous descending motion over the Indian
371 monsoon region (Fig.6c). Therefore, the biennial monsoon transitions between the
372 Indian and Australian summer monsoons during P1 can be established by the biennial
373 component of the ENSO with some contributions from Indian Ocean SSTs. SST
374 anomalies in the Atlantic Ocean are not involved in these Indian-Australian monsoon
375 transitions.

376 As for the biennial monsoon transition during P2, it consists of an

377 out-of-phase W-to-A transition and an in-phase A-to-W transition. The SST anomalies
378 composited for the W-to-A transition (Figs. 3e-h) are characterized by a developing
379 La Niña in the Pacific, an IOD and a basin-wide cooling in the Indian Ocean, and a
380 warming in the tropical Atlantic. The SST anomalies in the Pacific and Indian sectors
381 are mostly similar to the anomalies composited for the I-to-A transition during P1 but
382 are very different in the Atlantic sector. The 850-hPa velocity potential anomalies
383 (Figs.4e-h) indicate that there are significant differences between the
384 ascending/descending anomalies associated with the Walker circulations during P2
385 and P1. Anomalous ascent occurred over the tropical Atlantic during the summer of
386 P2 (Fig.4f) that was not observed during P1 (Fig.4b). The ascending anomalies above
387 the Indian region during P1 are displaced southeastward during P2 (Fig.4f), as a result
388 the rainfall anomalies in the Indian monsoon region became weaker (Fig.4f). In the
389 Pacific, the descending anomalies extend further westward during P2 (Fig.4f),
390 inducing low-level anticyclonic circulation anomalies (Fig.3f) that suppress the WNP
391 monsoon rainfall (Fig.4f).

392 Previous studies (*Kucharski et al. 2007, 2008; Wang et al. 2009; Cash et al.*
393 *2013*) have shown that warm tropical Atlantic SST anomalies can excite atmospheric
394 wave responses over the Indian Ocean that can weaken the Indian summer monsoon.
395 This weakening effect from the tropical Atlantic can cancel out the strengthening
396 effect produced by the developing La Niña. This cancelling has been verified in
397 numerical modeling experiments by *Kucharski et al. (2007)*. This cancelling should
398 also reduce the interannual variability of Indian monsoon during P2, which is
399 confirmed by a running variance analysis (see Fig.7). Thus, the increased influence of
400 the tropical Atlantic SST anomalies seems to be the reason why similar Indo-Pacific
401 SST anomalies can support a strong I-to-A transition during P1 but not during P2.

402 While they cancel out the La Niña influences on the Indian summer monsoon
403 variability, the tropical Atlantic SST anomalies can at the same time reinforce the La
404 Niña influence on the WNP summer monsoon variability. *Hong et al.* (2014) have
405 shown that warm tropical Atlantic SST anomalies can intensify the WNP subtropical
406 high and weaken the WNP summer monsoon via an anomalous zonally overturning
407 circulation, which ascends over the tropical Atlantic and descends over the equatorial
408 central Pacific. This anomalous descending motion can then excite a low-level
409 anticyclonic anomaly to the west and therefore weaken the WNP monsoon. Also, it is
410 known that negative SST anomalies in the tropical central Pacific associated with the
411 La Niña can weaken the WNP monsoon during boreal summer by inducing
412 anticyclonic circulation anomalies through a Gill-type response (*Gill* 1980; *Gu et al.*
413 2010). Thus, the tropical Atlantic SSTs and Pacific La Niña reinforce each other to
414 produce large negative anomalies in the WNP summer monsoon. Due to this
415 reinforcing effect, the intensity of the interannual variability in the WNP monsoon
416 was observed to increase markedly (Fig.7) during the P2 period. During DJF, Figs.
417 3g-h show that the tropical Atlantic SST anomalies decay while the Pacific La Niña
418 continues to grow and support a strong Australian summer monsoon. Therefore, the
419 Pacific La Niña and tropical Atlantic SST anomalies together support a transition
420 from a weak WNP summer monsoon in JJA to a strong Australian summer monsoon
421 in DJF (i.e., an out-of-phase W-to-A transition) during P2.

422 For the in-phase A-to-W transition during P2, the composite SST anomalies
423 (Figs. 5e-h) evolve from a decaying La Niña in DJF to a developing El Niño in JJA,
424 which is similar to the composite SST anomalies observed for the out-of-phase A-to-I
425 transition (see Figs. 5a-d). However, the A-to-W transition during P2 is associated
426 with significant SST anomalies in the tropical Atlantic during the transition seasons

427 (i.e., from DJF to the subsequent JJA). The tropical Atlantic cold SST anomalies again
428 act to cancel out the effect of the Pacific El Niño on the Indian monsoon (*Kucharski et*
429 *al. 2007*) but reinforce the El Niño influence on the WNP monsoon (*Hong et al. 2014*).
430 The 850-hPa circulation (Fig.5g) and rainfall anomalies (Fig.6g) also confirm that the
431 most active summer monsoon center during P2 is the WNP monsoon rather than the
432 Indian monsoon. Notable anomalous descent occurred over the tropical Atlantic
433 during the JJA of P2 (Fig.6g), in association with cold SST anomalies in the tropical
434 Atlantic (Fig.5g). These anomalies were not observed during P1 (Fig.6c). The region
435 of anomalous descent over the Indian Ocean moved off the Indian Peninsula during
436 P2 (Fig.6g). In the Pacific, anomalous ascent expanded westward greatly during P2
437 (Fig. 6g). These changes in ascending/descending anomalies lead to a shift of the
438 monsoon anomaly center from the Indian summer monsoon to the WNP monsoon.
439 These analyses indicate that Pacific and Atlantic SST anomalies together support a
440 transition from a strong Australian summer monsoon to a strong WNP summer
441 monsoons (i.e., an in-phase A-to-W transition) during P2.

442 One important feature to note from the SST composite analyses is that the
443 Pacific Ocean SST anomalies during the TBO monsoon transitions tend to be
444 accompanied by Indian Ocean SST anomalies of the same sign during P1 but with
445 Atlantic Ocean SST anomalies of the opposite sign during P2. To further confirm this
446 impression, we performed a correlation analysis of the tropical SST anomalies with
447 the JJA Niño3.4 index. As shown in Fig. 8a, the significant correlation coefficients are
448 characterized by an El Niño in the Pacific and an IOD in the Indian Ocean during P1.
449 El Niño during this period has little correlation with Atlantic SST anomalies. In
450 contrast, the significant correlation coefficients during P2 show that the El Niño in the
451 Pacific is accompanied by cold tropical Atlantic SST anomalies (Fig.8b). The

452 correlation with the Indian Ocean SST is very small. A sliding correlation analysis
453 also indicates a weakened correlation between the Niño3.4 index and the Indian DMI
454 index after the early 1990s (Fig.9a) but enhanced correlations between the Niño3.4
455 index and North and South Atlantic SST indices (Figs.9b,c). These results suggest that
456 there was a stronger Pacific-Indian Ocean coherence/coupling during P1 and a
457 stronger Pacific-Atlantic coherence/coupling during P2. Associated with the changes
458 in the inter-basin SST correlations, differences were observed in the ascending and
459 descending branches of the Walker circulations between these two periods (Fig.8).
460 Anomalous ascent and descent were confined within the Indo-Pacific regions during
461 P1 (Fig.8a) but extended into the Atlantic during P2 (Fig.8b). During the latter period,
462 anomalous descent developed over the tropical Atlantic where cold anomalies
463 occurred. At the same time, the descent anomalies over the Indian Ocean moved
464 southwestward leading to a decrease in their influence on the Indian summer monsoon,
465 whereas the ascent anomalies in the Pacific expanded westward leading to an increase
466 in their influence on the WNP summer monsoon. Therefore, the shift from the strong
467 Pacific-Indian Ocean coupling to the strong Pacific-Atlantic coupling may support the
468 shift of biennial monsoon transitions from the Indian-Australian monsoon transitions
469 to the WNP-Australian monsoon transitions. The stronger Pacific-Atlantic coupling
470 during recent decades is the primary reason why we observe a shift in the monsoon
471 centers in the biennial monsoon transitions associated with the TBO.

472 Consistent with the shift in biennial monsoon transitions from the
473 Indian-Australian monsoons during P1 to the WNP-Australian monsoons during P2,
474 stronger biennial variability is observed in the power spectrum of the Indian monsoon
475 during P1 but in the power spectrum of the WNP monsoon during P2 (Figs. 10a,b).
476 For the Australian monsoon, relatively strong biennial variability is found during both

477 P1 and P2 (Fig. 10c).

478

479 **5. Summary and discussion**

480 In this study, we performed statistical analyses using observations and
481 reanalysis products to show that two important changes to the TBO have occurred
482 since the early 1990s: (1) the biennial monsoon transitions associated with the TBO
483 have shifted from involving the Indian-Australian summer monsoons to involving the
484 WNP-Australian summer monsoons, and (2) tropical Atlantic SST anomalies have
485 become an important part of the monsoon-ocean interactions associated with the TBO.
486 Figure 11 illustrates how the different SST anomaly patterns before and after the early
487 1990s can induce the shift of the summertime monsoon centers. During the period
488 before the early-1990s, strong Pacific-Indian SST coupling/coherence confined most
489 of the anomalous ascent/descent to the Indo-Pacific region (Fig.11a), with one of the
490 anomaly centers located right over the Indian monsoon region. During the period after
491 the early-1990s, strong Pacific-Atlantic SST coupling/coherence displaced the
492 locations of the anomalous ascent/descent centers and shifted one center to the WNP
493 monsoon region (Fig.11b). Therefore, the changes in the monsoon centers associated
494 with the TBO are related to an increased influence of tropical Atlantic SST anomalies
495 on the Indian and WNP summer monsoons. The increased Atlantic SST influence acts
496 to weaken the ENSO influence on the Indian summer monsoon leading to a decrease
497 in its variability but enhances the ENSO influence on the WNP summer monsoon to
498 increase its variability (Fig.11c). As a result, during the last two decades the WNP
499 monsoon has replaced the Indian monsoon to become a major component in the
500 biennial monsoon transitions associated with the TBO. These results highlight the
501 important roles of Pacific-Atlantic interactions in the TBO dynamics in recent
502 decades.

503 Much effort has been expended attempting to understand the TBO dynamics,
504 most of which involve interactions between the Indian-Australian summer monsoons
505 and SST anomalies in the Indo-Pacific sector (e.g., *Meehl*, 1987, 1993; *Chang and Li*
506 2000; *Loschnigg et al.* 2003; *Yu et al.* 2003; *Meehl et al.* 2003). Our results suggest
507 that the Pacific-Atlantic Ocean sector may have become involved in the TBO
508 dynamics after the early-1990s, in contrast to the pre-1990s TBO dynamics that
509 mainly involved the Pacific-Indian Ocean sector (e.g., *Chang and Li* 2000; *Meehl et*
510 *al.* 2003; *Yu et al.* 2003; *Loschnigg et al.* 2003). This shift in the TBO dynamics may
511 be part of the early-1990s climate shift (*Qian et al.* 2014; *Yu et al.* 2015; *Paek et al.*
512 2016; *Lyu et al.* 2017; *Wang et al.* 2017) that has been linked to a phase change of the
513 AMO and global warming trends. The main message of this study is that the TBO and
514 its underlying dynamics may have to be studied separately for the periods before and
515 after the early-1990s.

516 The change in the biennial monsoon transitions associated with the TBO
517 during the recent two decades may affect the strategies used for seasonal climate
518 predictions in the Asian-Australian monsoonal regions. For example, tropical Atlantic
519 SSTs may need to be considered and incorporated more than previously when
520 predicting the Asian-Australian monsoon. Also, the characteristics of the Australian
521 summer monsoon may become more useful for predicting the WNP summer monsoon
522 during the following boreal summer. Since the intensity of the EA summer monsoon
523 generally has a negative correlation with that of the WNP summer monsoon (e.g.,
524 *Kwon et al.* 2005), a better prediction of the WNP summer can also benefit predictions
525 of the EA summer monsoon that is closely associated with the Chinese Mei-yu, the
526 Korean Changma, and the Japanese Baiu.

527 Our results suggest an increase in the importance of Pacific-Atlantic

528 interactions to the TBO dynamics in recent decades, at around the time when the
529 AMO changed from a negative to a positive phase (in the early-1990s). The phase of
530 the AMO may be playing a role in the increased influence of the Atlantic during some
531 decades but not others. Different phases of the AMO may produce different
532 inter-basin SST gradients between the Pacific and Atlantic and different impacts on
533 the strengths of Walker circulations above the basins (*Wang 2006; Chikamoto et al.*
534 *2015; Zhang and Karneuskas 2017*), which may separately or together affect the role
535 of the Atlantic Ocean in the TBO dynamics. Further studies are needed to better
536 understand these inter-basin interaction processes.

537

538

539 **Acknowledgments**

540 We thank the three anonymous reviewers for their comments and suggestions that
541 have greatly improved the manuscript. This work was supported by the National
542 Science Foundation's Climate and Large Scale Dynamics Program under Grant
543 AGS-1505145. L.W.'s work was also supported by the National Natural Science
544 Foundation of China (Grant No.41776031), the Guangdong Natural Science
545 Foundation (Grant No.2015A030313796), and the National Program on Global
546 Change and Air-Sea Interaction (GASI-IPOVAI-04). L.W. thanks the China
547 Scholarship Council for supporting his visit to the University of California, Irvine.

- 549 Cai, W. and P. van Rensch, 2013: Austral summer teleconnections of Indo-Pacific
550 variability: their nonlinearity and impacts on Australian climate. *J. Climate*, **26**,
551 2796-2810.
- 552 Cash, B.A., X. Rodo, J. Ballester, M.J. Bouma, A. Baeza, R. Dhiman, and M.
553 Pascual, 2013: Malaria epidemics and the influence of the tropical South Atlantic
554 on the Indian monsoon. *Nature Clim. Change*, **3**, 502-507.
- 555 Chang, C.P., and T. Li, 2000: A theory for the tropical tropospheric biennial
556 oscillation. *J. Atmos. Sci.*, **57**, 2209–2224.
- 557 Chen, M., P. Xie, J. E. Janowiak, and P. A. Arkin, 2002: Global Land Precipitation:
558 A 50-yr monthly analysis based on gauge observations. *J. of Hydrometeorology*,
559 **3**, 249-266.
- 560 Chikamoto, Y., A. Timmermann, J.-J. Luo, T. Mochizuki, M. Kimoto, M. Watanabe,
561 M. Ishii, S.P. Xie, F.F. Jin, 2015: Skilful multi-year predictions of tropical
562 trans-basin climate variability. *Nat. Commun.*, **6**:6869.doi:10.1038/ncomms7869.
- 563 Clarke, A. J., X. Liu, and S. V. Gorder, 1998: Dynamics of the biennial oscillation in
564 the equatorial Indian and far western Pacific Oceans. *J. Climate*, **11**, 987–1001.
- 565 Gill, A. E, 1980: Some simple solutions for the heat induced tropical circulation.
566 *Quart. J. Meteorol. Soc.*, **106**, 447-462.
- 567 Gu, D., T. Li, Z. Li, and B. Zheng, 2010: On the phase relations between the Western
568 North Pacific, Indian, and Australian monsoons. *J. Climate*, **23**, 5572–5589.
- 569 Hong, C.C., T.C. Chang, and H.H. Hsu, 2014: Enhanced relationship between the
570 tropical Atlantic SST and the summertime western North Pacific subtropical high
571 after the early 1980s. *J. Geophys. Res. Atmos.*, **119**, 3715–3722.
- 572 Hung, C.W., X. D. Liu, and M. Yanai, 2004: Symmetry and asymmetry of the Asian
573 and Australian summer monsoons. *J. Climate*, **17**, 2413–2426.
- 574 Kalnay, E., and Coauthors, 1996: The NCEP/NCAR 40-Year Reanalysis Project.
575 *Bull. Amer. Meteor. Soc.*, **77** (3), 437–471.
- 576 Kajikawa, Y., B. Wang, and J. Yang, 2010: A multi-time scale Australian monsoon
577 index. *Int. J. Climatol.*, **30**, 1114–1120.
- 578 Kao, H.Y., and J.Y. Yu, 2009: Contrasting eastern Pacific and central Pacific types of
579 ENSO. *J. Climate*, **22**, 615–632.
- 580 Keenlyside, N. S., H. Ding, and M. Latif, 2013: Potential of equatorial Atlantic
581 variability to enhance El Niño prediction. *Geophys. Res. Lett.*, **40**, 2278–2283,
582 doi:10.1002/grl.50362.
- 583 Kerr, R. A., 2000: A North Atlantic climate pacemaker for the centuries. *Science*, **288**,
584 1984–1986, doi:10.1126/science.288.5473.1984.
- 585 Kiladis, G.N. and H. van Loon, 1988: The Southern Oscillation. Part VII:
586 Meteorological anomalies over the Indian and Pacific sectors associated with the
587 extremes of the oscillation. *Mon. Wea. Rev.*, **116**, 120-136.
- 588 Kucharski, F., A. Bracco, J. H. Yoo, and F. Molteni, 2007: Low-frequency variability
589 of the Indian monsoon–ENSO relationship and the tropical Atlantic: the

590 'weakening' of the 1980s and 1990s. *J. Climate*, **20**, 4255– 4266.

591 Kucharski, F., A. Bracco, J. H. Yoo, and F. Molteni, 2008: Atlantic forced
592 component of the Indian monsoon interannual variability. *Geophys. Res. Lett.*,
593 **35**, L04706, doi:10.1029/2007GL033037.

594 Kwon, M.,J.-G.Jhun, B. Wang, S.-I. An, and J.-S.Kug, 2005: Decadal change in
595 relationship between east Asian and WNP summer monsoons. *Geophys. Res.*
596 *Lett.*, **32**, L16709, doi:10.1029/2005GL023026.

597 Lau,K.-M.and S. Yang, 1996: The Asian monsoon and predictability of the tropical
598 ocean–atmosphere system. *Quart. J. Roy. Meteor. Soc.*, **122**, 945–957.

599 Lee, E.-J., K.-J. Ha, and J.-G. Jhun, 2014: Interdecadal changes in interannual
600 variability of the global monsoon precipitation and interrelationships among its
601 subcomponents. *Clim. Dyn.*, **42**, 2585-2601.

602 Li, T., P. Liu, X. Fu, B. Wang and G.A. Meehl, 2006: Spatiotemporal structures and
603 mechanisms of the tropospheric biennial oscillation in the Indo-Pacific Warm
604 Ocean regions. *J. Climate*, **19**, 3070–3087.

605 Li, X., S.P. Xie, S.T. Gille, and C. Yoo, 2016: Atlantic-induced pan-tropical climate
606 change over the past three decades. *Nature Clim. Change*, **6**, 275-279.

607 Loschnigg, J., G.A. Meehl, P.J. Webster, J.M. Arblaster, and G.P. Compo, 2003: The
608 Asian monsoon, the tropospheric biennial oscillation and the Indian Ocean zonal
609 mode in the NCAR CSM. *J. Climate*, **16**, 2138-2158.

610 Lyu, K., J.Y. Yu and H. Paek, 2017: The influences of the Atlantic Multidecadal
611 Oscillation on the Mean Strength of the North Pacific Subtropical High during
612 Boreal Winter. *J. Climate*, **30**, 411-426.

613 Matsumoto, J., 1992: The seasonal changes in Asian and Australian regions. *J.*
614 *Meteor. Soc. Japan*, **70**, 257–273.

615 Meehl, G. A., 1987: The annual cycle and interannual variability in the tropical
616 Pacific and Indian Ocean region. *Mon. Wea. Rev.*, **115**, 27–50.

617 Meehl, G. A., 1993: A coupled air-sea biennial mechanism in the tropical Indian and
618 Pacific regions: Role of the ocean. *J. Climate*, **6**, 31-41.

619 Meehl, G. A., 1994: Coupled land–ocean–atmosphere processes and south Asian
620 monsoon variability. *Science*, **266**, 263–267.

621 Meehl, G.A., 1997: The South Asian monsoon and tropospheric biennial oscillation.
622 *J. Climate*, **10**, 1921–1943.

623 Meehl, G. A. and J. M. Arblaster, 2002a: The tropospheric biennial oscillation and
624 Asian–Australian monsoon rainfall. *J. Climate*, **15**, 722–744.

625 Meehl, G. A. and J. M. Arblaster, 2002b: Indian monsoon GCM experiments testing
626 tropospheric biennial oscillation transition conditions. *J. Climate*, **15**, 923–944.

627 Meehl, G. A., J. M. Arblaster, and J. Loschnigg, 2003: Coupled-ocean-atmosphere
628 dynamical processes in tropical Indian and Pacific oceans and the TBO. *J.*
629 *Climate*, **16**, 2138–2158.

630 Nicholls, N., 1978: Air–sea interaction and the quasi-biennial oscillation. *Mon. Wea.*
631 *Rev.*, **106**, 1505–1508.

632 Nicholls, N.,1979: A simple air–sea interaction model. *Quart. J. Roy. Meteor. Soc.*,
633 **105**, 93–105.

634 Nicholls, N., 1984: The Southern Oscillation and Indonesian sea-surface
635 temperature. *Mon. Wea. Rev.*, **112**, 424–432.

636 Paek, H., J.Y. Yu , F. Zheng, and M.M. Lu, 2016: Impacts of ENSO Diversity on the
637 Western Pacific and North Pacific Subtropical Highs during Boreal Summer.
638 *Clim.Dyn.*, DOI: 10.1007/s00382-016-3288-z.

639 Qian, C., J.Y. Yu, and G. Chen, 2014: Decadal Summer Drought Frequency in
640 China: The increasing influence of the Atlantic Multi-decadal Oscillation.
641 *Environ. Res. Lett.*, **9(12)**, 124004.

642 Rasmusson, E. M., and T. H. Carpenter, 1983: The relationship between the eastern
643 Pacific sea surface temperature and rainfall over India and Sri Lanka. *Mon. Wea.*
644 *Rev.*, **111**, 517–528.

645 Rodionov, S. N. ,2004: A sequential algorithm for testing climate regime shifts.
646 *Geophys. Res. Lett.*, 31, L09204, doi:10.1029/2004GL019448.

647 Rodríguez-Fonseca, B., I. Polo, J. García-Serrano, T. Losada, E. Mohino, C. R.
648 Mechoso, and F. Kucharski, 2009: Are Atlantic Niños enhancing Pacific ENSO
649 events in recent decades? *Geophys. Res. Lett.*, 36, L20705,
650 doi:10.1029/2009GL040048.

651 Ropelewski, C. F., M. S. Halpert, and X. Wang, 1992: Observed tropospheric
652 biennial variability and its relationship to the Southern Oscillation. *J. Climate*, **5**,
653 594–614.

654 Saji, N.H., B.N.Goswami, P. N. Vinayachandran, and T. Yamagata, 1999: A dipole
655 mode in the tropical Indian Ocean. *Nature*, **401**,360–363.

656 Schlesinger, M. E., and N. Ramankutty, 1994: An oscillation in the global climate
657 system of period 65-70 years. *Nature*, **367**, 723–726, doi:10.1038/367723a0.

658 Smith, T. M., R. W. Reynolds, T. C. Peterson, and J. Lawrimore, 2008:
659 Improvements to NOAA’s historical merged land-ocean surface temperature
660 analysis (1880–2006). *J. Climate*, **21**, 2283-2296.

661 Sui, C.-H., P.-H. Chung, and T. Li, 2007: Interannual and interdecadal variability of
662 the summertime western North Pacific subtropical high. *Geophys. Res. Lett.*, **34**,
663 L11701, doi:10.1029/2006GL029204.

664 Taschetto, A.S., G.A. Sen, H.H. Hendon, C.C. Ummenhofer, and M.H. England,
665 2011: The contribution of Indian Ocean sea surface temperature anomalies on
666 Australian summer rainfall during El Niño events. *J. Climate*, **24**, 3734–3747.

667 Wang, B. and Z. Fan, 1999: Choice of South Asian summer monsoon indices. *Bull.*
668 *Amer. Meteor. Soc.*, **80**, 629–638.

669 Wang, B., R. Wu, and K.M. Lau, 2001: Interannual variability of Asian summer
670 monsoon: Contrast between the Indian and western North Pacific-East Asian
671 monsoons. *J. Climate*, **14**, 4073-4090.

672 Wang, C., 2006: An overlooked feature of tropical climate: Inter-Pacific-Atlantic
673 variability. *Geophys. Res. Lett.*, 33, L12702, doi:10.1029/2006GL026324.

674 Wang, C., F. Kucharski, R. Barimalala, and A. Bracco, 2009: Teleconnections of the
675 tropical Atlantic to the tropical Indian and Pacific oceans: A review of recent
676 findings. *Meteorol. Z.*, **18**, 445–454, doi:10.1127/0941-2948/2009/0394.

677 Wang, L., J.Y. Yu, and H. Paek, 2017: Enhanced biennial variability in the Pacific
678 due to Atlantic capacitor effect. *Nat. Commun.*, **8**, 14887 doi:
679 10.1038/ncomms14887.

680 Webster, P. J., A. M. Moore, J. P. Loschnigg, and R. R. Leben, 1999: Coupled
681 oceanic-atmospheric dynamics in the Indian Ocean during 1997-98. *Nature*, **401**,
682 356–360.

683 Wu, R. and B.P. Kirtman, 2004: The tropospheric biennial oscillation of the
684 monsoon-ENSO system in an interactive ensemble coupled GCM. *J. Climate*,
685 **17**, 1623–1640.

686 Yu, J.Y., S.P. Weng, and J.D. Farrara, 2003: Ocean roles in TBO transition of
687 Indian-Australian monsoon system. *J. Climate*, **16**, 3072–3080.

688 Yu, J.Y., and H.Y. Kao, 2007: Decadal changes of ENSO persistence barrier in SST
689 and ocean heat content indices: 1958–2001. *J. Geophys. Res.*, **112**, D13106,
690 doi:10.1029/2006JD007654.

691 Yu, J.Y., M.M. Lu, and S. T. Kim, 2012: A change in the relationship between
692 tropical central Pacific SST variability and the extratropical atmosphere around
693 1990. *Environ. Res. Lett.*, **7**, 034025, doi:10.1088/1748-9326/7/3/034025.

694 Yu, J.Y., P.K. Kao, H. Paek, H.H. Hsu, C.W. Hung, M.M. Lu, and S.I. An, 2015:
695 Linking emergence of the central-Pacific El Niño to the Atlantic Multi-decadal
696 Oscillation. *J. Climate*, **28**, 651-662.

697 Zhang, L. and K.B. Karnauskas, 2017: The role of tropical interbasin SST gradients
698 in forcing Walker circulation trends. *J. Climate*, **30**, 499-508.

699 Zheng, B., D. J. Gu, A. L. Lin, and C. H. Li, 2008: Spatial patterns of tropospheric
700 biennial oscillation and its numerical simulation. *Adv. Atmos. Sci.*, **25(5)**,
701 815–823.

702

703

704

705

706

707

708

709

710

711

712

713

714

715

716 **Table caption**

717 Table 1. Comparison of the correlations between the Indian/WNP and Australian
718 monsoon indices during P1 and P2. Correlations that are significant at the 95%
719 confidence level are shown in boldface.

720

721 Table 2. Selected cases of monsoon transitions during P1 (I-to-A and A-to-I
722 transitions) and P2 (W-to-A and A-to-W transitions). The years are shown are the
723 years of the JJA Indian monsoon or the JJA WNP monsoon involved in the transitions.

724

725 **Figure captions**

726 Figure 1.(a) The 21-year sliding correlation coefficients (e.g., the correlation
727 coefficient in 2000 represents the period 1990–2010) between the JJA Indian monsoon
728 index and the DJF Australian monsoon index for the period 1948–2016. (b) Same as
729 (a) but for the JJA WNP monsoon index and the DJF Australian monsoon index. The
730 red (yellow) dots in (a) and (b) represent correlations that are significant at the 95%
731 (90%) confidence level. (c) The BTI between the JJA Indian/WNP monsoon and the
732 DJF Australian monsoon.

733

734 Figure 2. Wavelet power spectrum of the summer monsoon indices for (a) WNP
735 monsoon, (b) Indian monsoon and (c) Australian monsoon. The regions exceeding the
736 95% confidence level against red noise are dotted.

737

738 Figure 3. Differences in SSTs (shading) and 850-hPa winds (vectors) between the
739 “positive” and “negative” monsoon composites from MAM to the following DJF for
740 the I-to-A transitions during P1 (a-d) and the W-to-A transitions during P2 (e-h). Only
741 the values at the 90% confidence level or higher are shown. The red circles in (b) and
742 (f) represent the summertime low-level circulation anomalies over the Indian/WNP
743 monsoon region, with A (C) denoting anticyclone (cyclone).

744

745 Figure 4. Same as Figure 3 but for the rainfall (shading) and 850-hPa velocity
746 potential (contours, $10^6 \text{ m}^2 \text{ s}^{-1}$, solid for positive and dashed for negative values).
747 The green boxes in (b) and (f) encompass the core regions of the Indian and WNP
748 monsoon according to Wang et al. (2001).

749

750 Figure 5. Differences in SSTs (shading) and 850-hPa winds (vectors) between the
751 “positive” and “negative” monsoon composites from DJF to the following SON for
752 the A-to-I transitions during P1 (a-d) and the A-to-W transitions during P2 (e-h). Only
753 the values at the 90% confidence level or higher are shown. The red circles in (c) and
754 (g) represent the summertime low-level circulation anomalies over the Indian/WNP
755 monsoon region, with A (C) denoting anticyclone (cyclone).

756

757 Figure 6. Same as Figure 5 but for the rainfall (shading) and 850-hPa velocity
758 potential (contours, $10^6 \text{ m}^2 \text{ s}^{-1}$, solid for positive and dashed for negative values).
759 The green boxes in (b) and (f) encompass the core regions of the Indian and WNP
760 monsoon according to Wang et al. (2001).

761

762

763 Figure 7. Time series of anomalies in the intensity of the interannual variations in the
764 three monsoon indices. The intensity of the interannual variations is defined as the
765 21-year running standard deviation of the interannual monsoon indices. The
766 anomalies are then calculated by subtracting the long-term mean intensity of the
767 interannual variations during the entire analysis period.

768

769 Figure 8. The correlations of the JJA Niño3.4 index with JJA SST (shading) and
770 850-hPa velocity potential (contours, solid for positive and dashed for negative
771 values) at each grid point (a) during P1 and (b) during P2. Only the values at the 90%
772 confidence level or higher are shown.

773

774 Figure 9. (a) The 21-year sliding correlation coefficients (e.g., the correlation
775 coefficient in 2000 represents the period 1990–2010) between the JJA Niño3.4 and
776 Indian DMI during 1948–2016. (b) Same as (a) but for the JJA Niño3.4 and tropical
777 South Atlantic SSTs. According to *Kucharski et al.* (2008), the warm tropical South
778 Atlantic SSTs could weaken the summer Indian monsoon. (c) Same as (a) but for the
779 JJA Niño3.4 and tropical North Atlantic SSTs. According to *Hong et al.* (2014), the
780 warm tropical North Atlantic SSTs could enhance the WNP subtropical high and
781 weaken the summer WNP monsoon. The red dots represent correlations that are
782 significant at the 95% confidence level.

783

784 Figure 10. Comparison of power spectrum for the monsoon indices before and after
785 the early 1990s. Distribution of power spectrum for (a) WNP monsoon, (b) Indian
786 monsoon and (c) Australian monsoon. The dashed line denotes the 95% confidence
787 interval against red noise.

788

789 Figure 11. A schematic diagram showing the physical processes to induce the recent
790 shift in the monsoon centers of the TBO. (a) The Pacific-Indian Ocean
791 coherence/coupling before the early 1990s supports the Indian summer monsoon to be
792 the monsoon center involved in the TBO. (b) The Pacific-Atlantic Ocean
793 coherence/coupling after the early 1990s supports the WNP summer monsoon to be
794 the monsoon center involved in the TBO. (c) The schematic summarizing the possible
795 influences of the Atlantic Ocean on the shift of the summertime monsoon centers
796 involved in the TBO.

797

798

Table 1. Comparison of the correlations between the Indian/WNP and Australian monsoon indices during P1 and P2. Correlations that are significant at the 95% confidence level are shown in boldface.

	P1 (1967-1987)	P2 (1994-2014)
JJA Indian monsoon and following DJF Australian monsoon	0.65	0.39
DJF Australian monsoon and subsequent JJA Indian monsoon	-0.54	-0.19
JJA WNP monsoon and following DJF Australian monsoon	0.15	-0.75
DJF Australian monsoon and subsequent JJA WNP monsoon	0.38	0.64

Table 2. Selected cases of monsoon transitions during P1 (I-to-A and A-to-I transitions) and P2 (W-to-A and A-to-W transitions). The years are shown are the years of the JJA Indian monsoon or the JJA WNP monsoon involved in the transitions.

	“Positive”	“Negative”
I-to-A (P1)	1967,1970,1973,1975,1980	1969,1972,1974,1987
A-to-I(P1)	1974,1981,1987	1970,1973,1975,1978,1983
W-to-A (P2)	1996,1998,2003,2007,2008,2010	1997,2004,2006,2009,2012
A-to-W (P2)	1997,2001,2004,2009	1998,2003,2007,2010

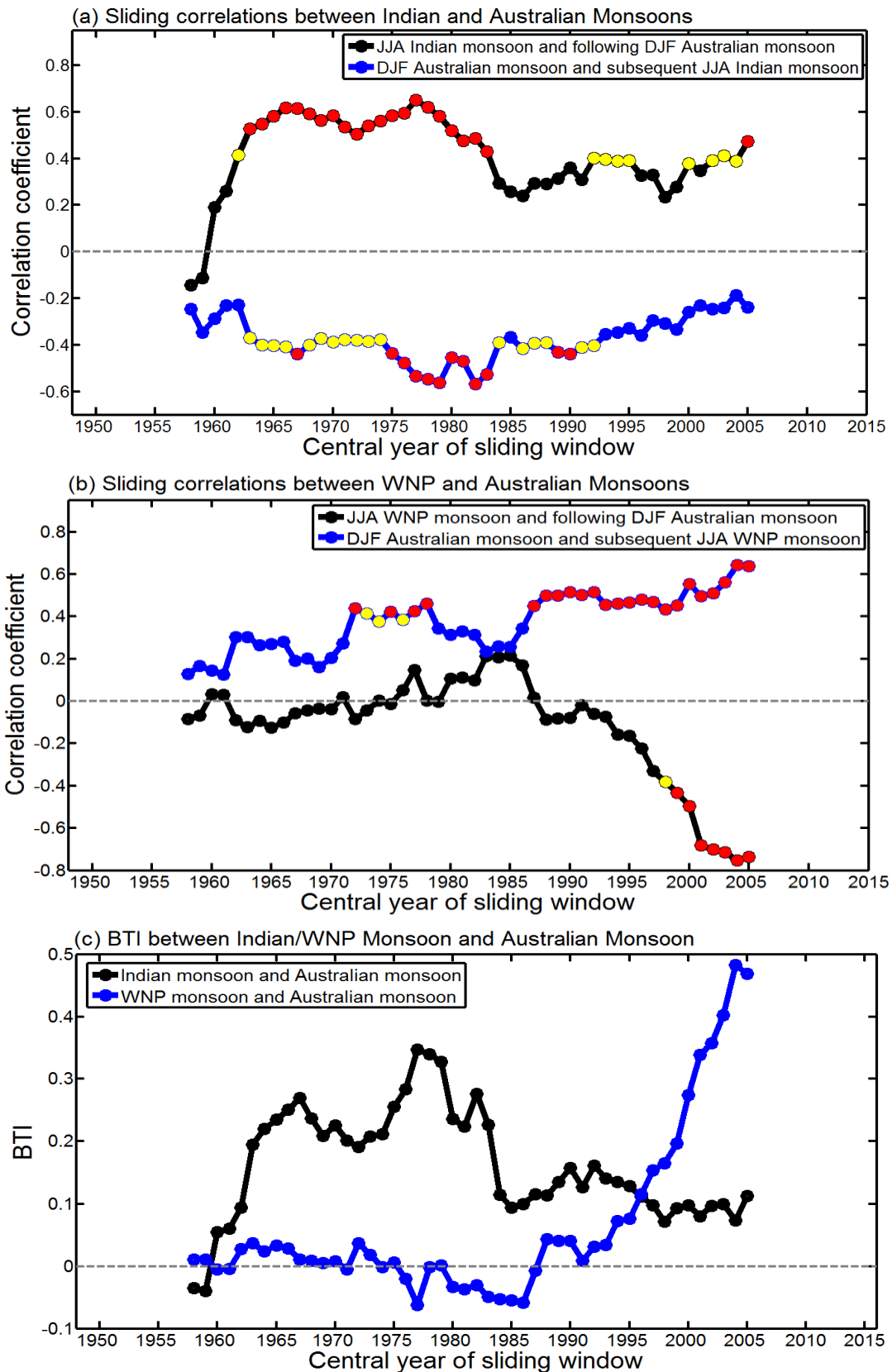


Figure 1.(a)The 21-year sliding correlation coefficients (e.g., the correlation coefficient in 2000 represents the period 1990–2010) between the JJA Indian monsoon index and the DJF Australian monsoon index for the period 1948–2016. (b) Same as (a) but for the JJA WNP monsoon index and the DJF Australian monsoon index. The red (yellow) dots in (a) and (b) represent correlations that are significant at the 95% (90%) confidence level. (c) The BTI between the JJA Indian/WNP monsoon and the DJF Australian monsoon.

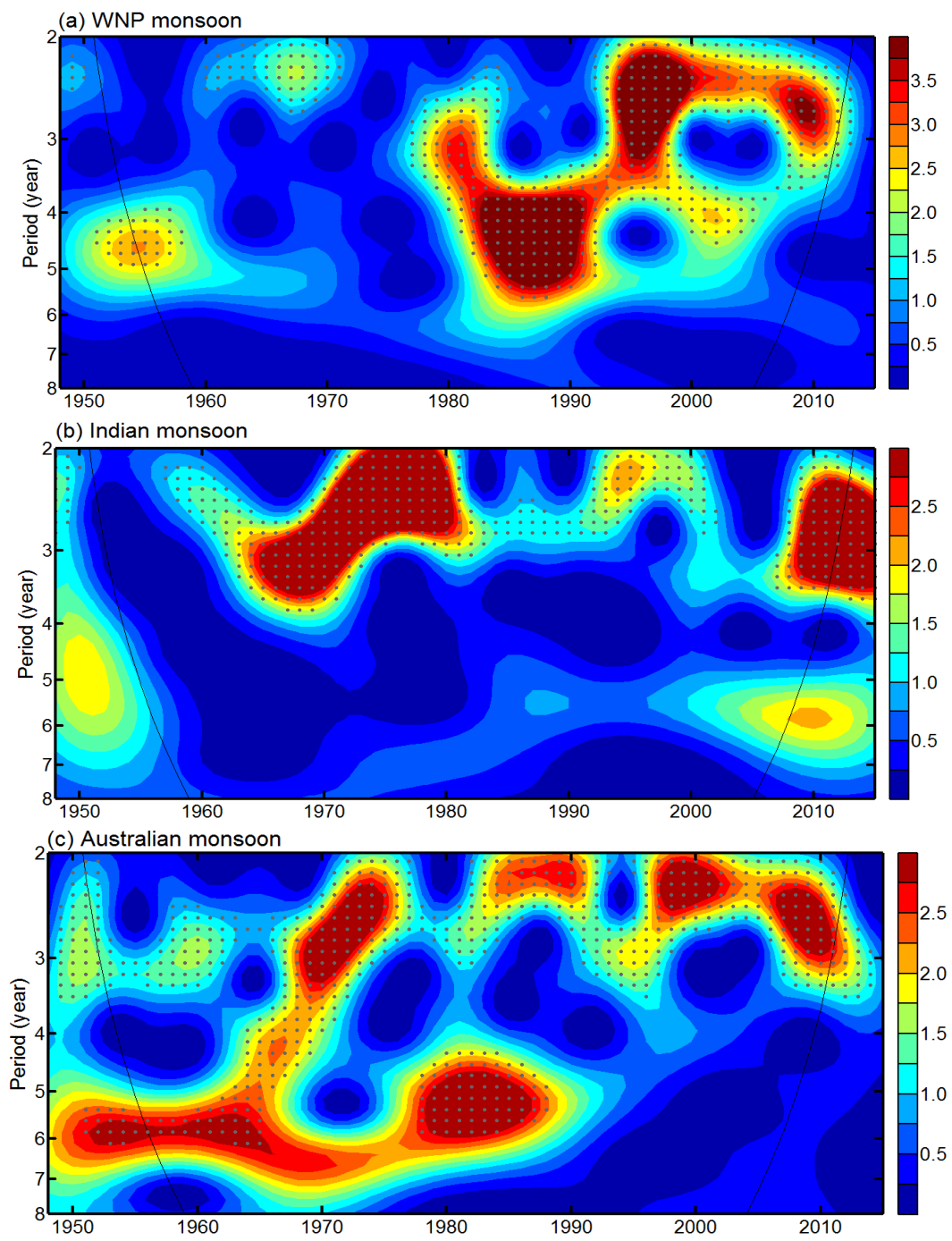


Figure 2. Wavelet power spectrum of the summer monsoon indices for (a) WNP monsoon, (b) Indian monsoon and (c) Australian monsoon. The regions exceeding the 95% confidence level against red noise are dotted.

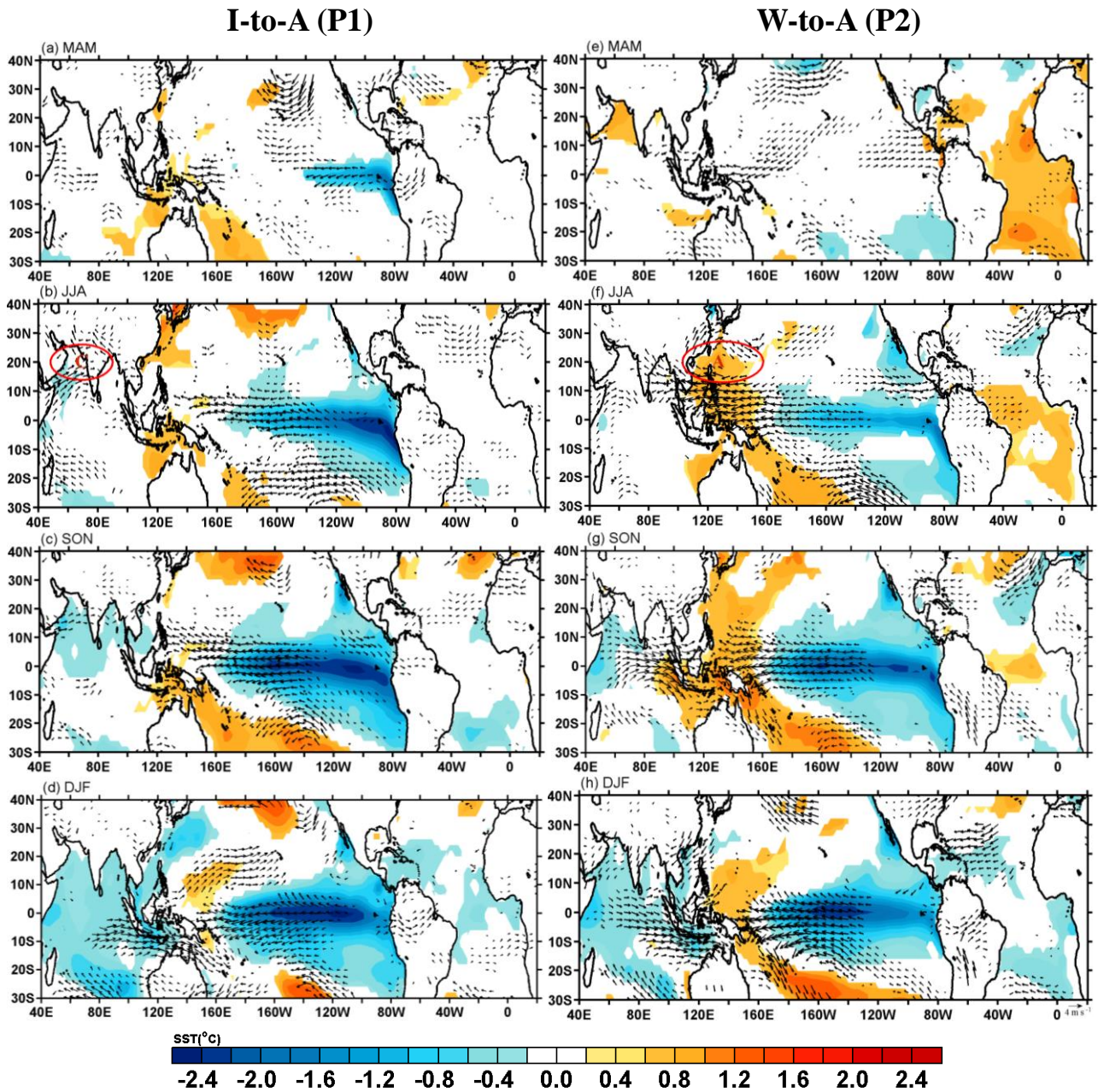


Figure 3. Differences in SSTs (shading) and 850-hPa winds (vectors) between the “positive” and “negative” monsoon composites from MAM to the following DJF for the I-to-A transitions during P1 (a-d) and the W-to-A transitions during P2 (e-h). Only the values at the 90% confidence level or higher are shown. The red circles in (b) and (f) represent the summertime low-level circulation anomalies over the Indian/WNP monsoon region, with A (C) denoting anticyclone (cyclone).

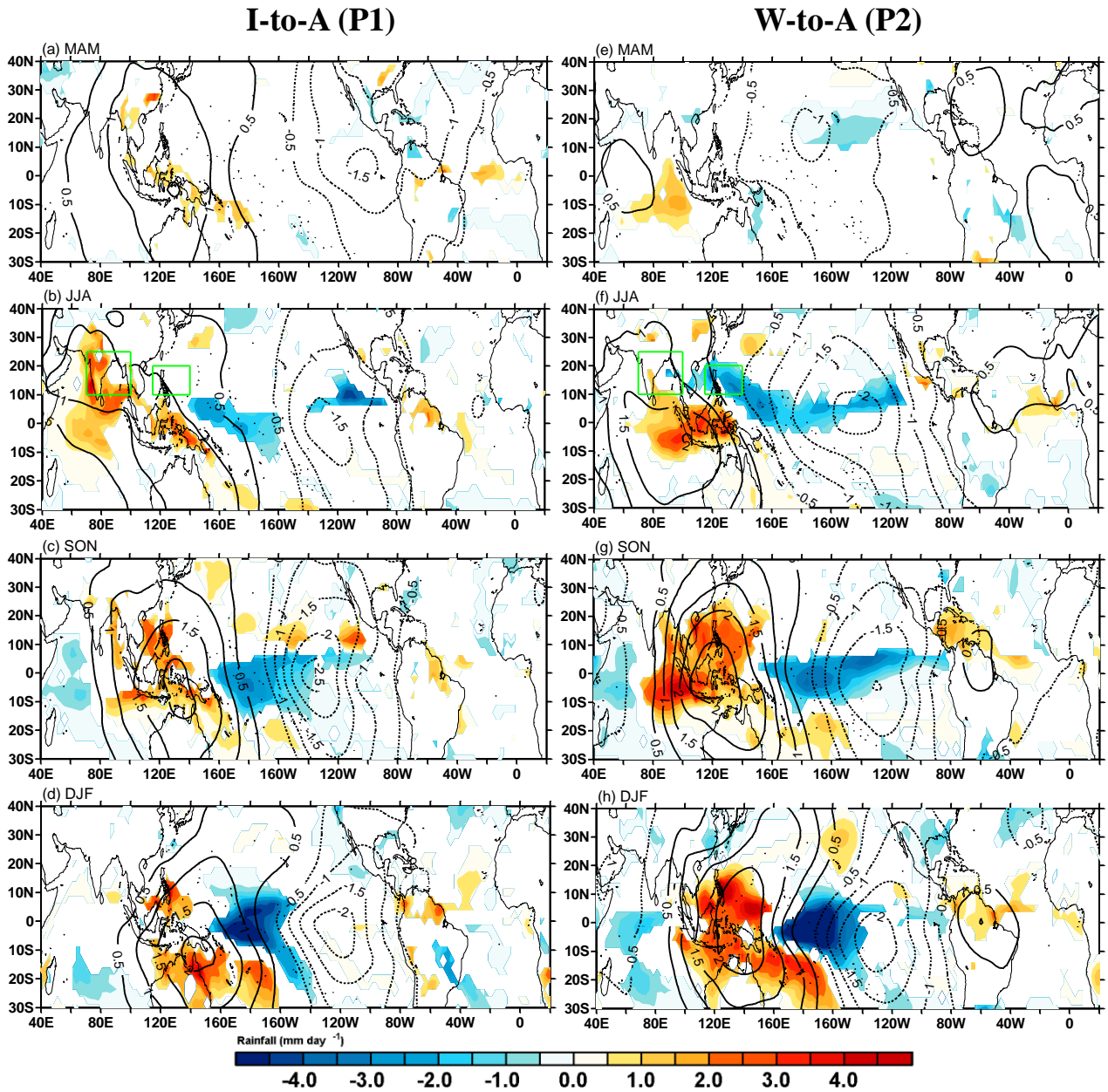


Figure 4. Same as Figure 3 but for the rainfall (shading) and 850-hPa velocity potential (contours, $10^6 \text{ m}^2 \text{ s}^{-1}$, solid for positive and dashed for negative values). The green boxes in (b) and (f) encompass the core regions of the Indian and WNP monsoon according to Wang et al. (2001).

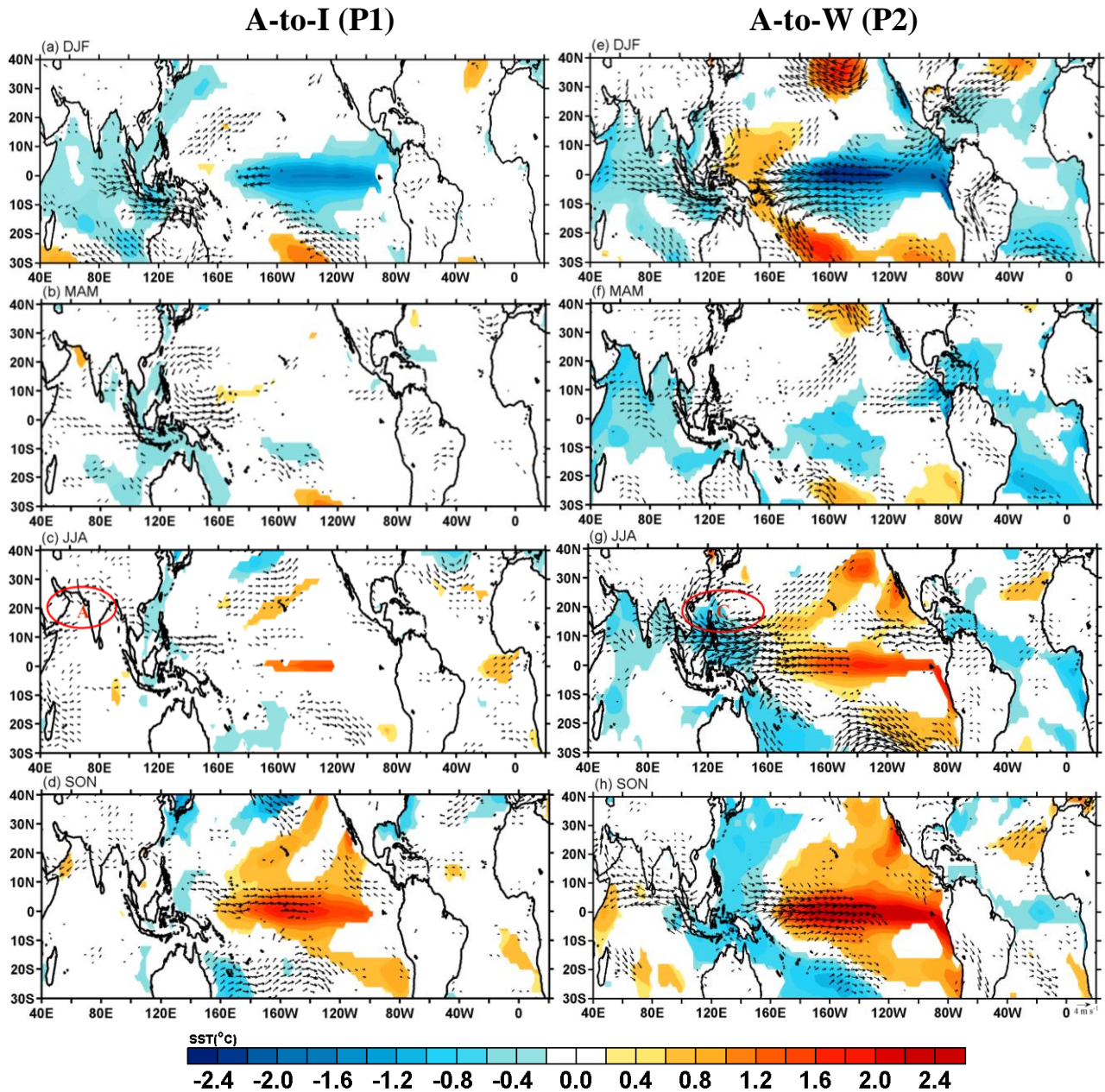


Figure 5. Differences in SSTs (shading) and 850-hPa winds (vectors) between the “positive” and “negative” monsoon composites from DJF to the following SON for the A-to-I transitions during P1 (a-d) and the A-to-W transitions during P2 (e-h). Only the values at the 90% confidence level or higher are shown. The red circles in (c) and (g) represent the summertime low-level circulation anomalies over the Indian/WNP monsoon region, with A (C) denoting anticyclone (cyclone).

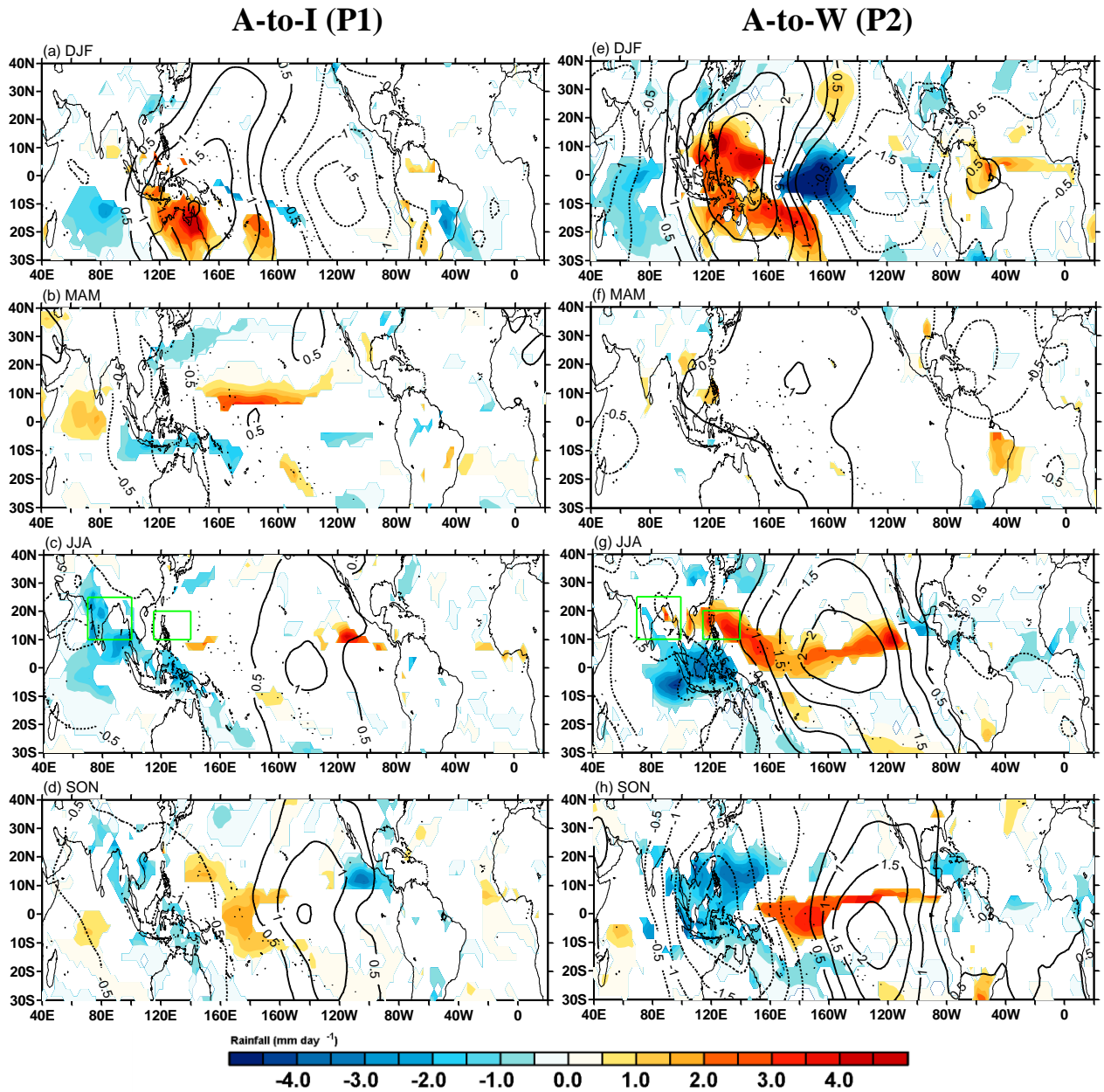


Figure 6. Same as Figure 5 but for the rainfall (shading) and 850-hPa velocity potential (contours, $10^6 \text{ m}^2 \text{ s}^{-1}$, solid for positive and dashed for negative values). The green boxes in (b) and (f) encompass the core regions of the Indian and WNP monsoon according to Wang et al. (2001).

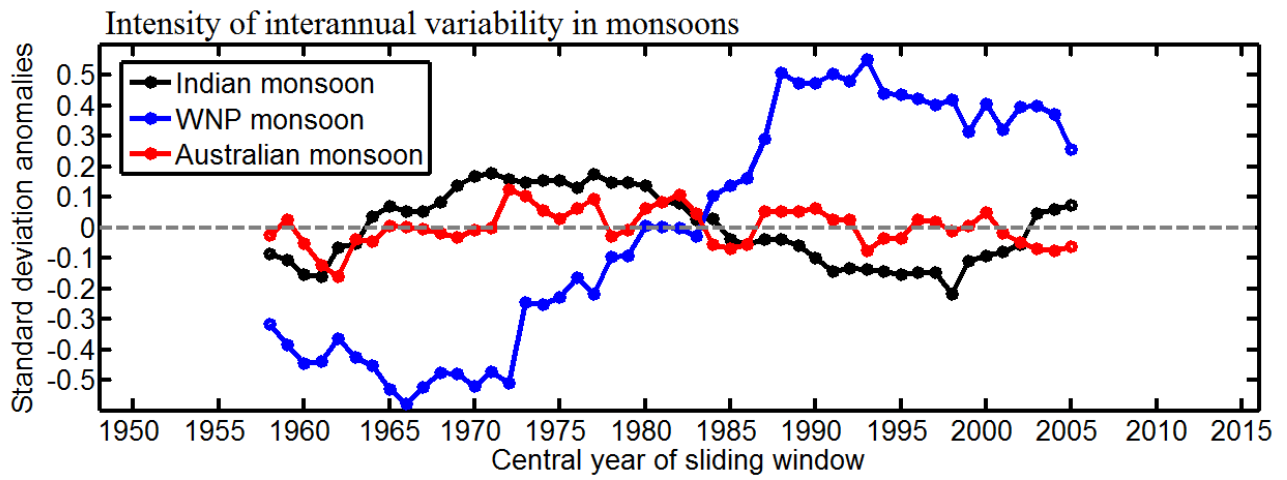


Figure 7. Time series of anomalies in the intensity of the interannual variations in the three monsoon indices. The intensity of the interannual variations is defined as the 21-year running standard deviation of the interannual monsoon indices. The anomalies are then calculated by subtracting the long-term mean intensity of the interannual variations during the entire analysis period.

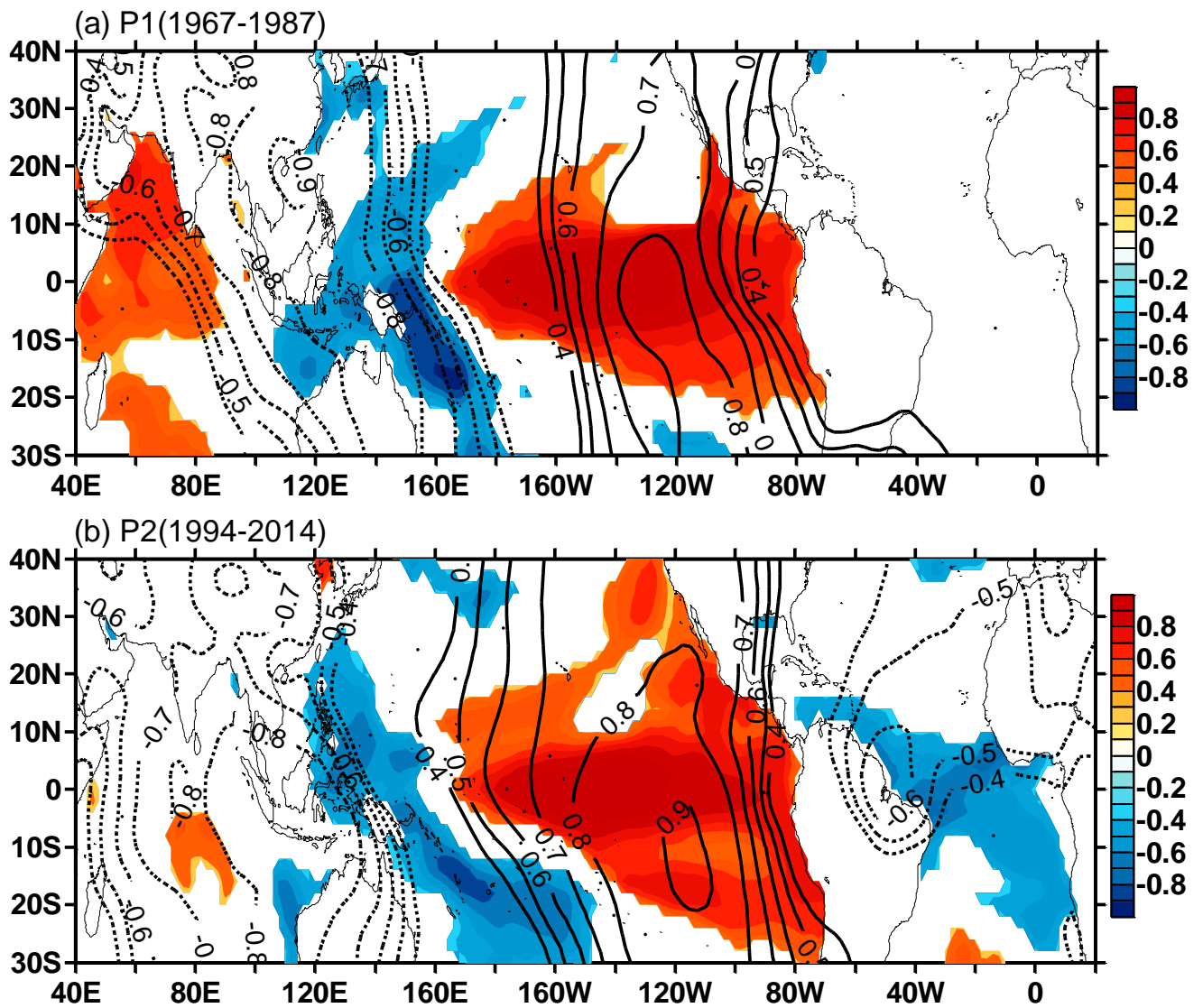


Figure 8. The correlations of the JJA Niño3.4 index with JJA SST (shading) and 850-hPa velocity potential (contours, solid for positive and dashed for negative values) at each grid point (a) during P1 and (b) during P2. Only the values at the 90% confidence level or higher are shown.

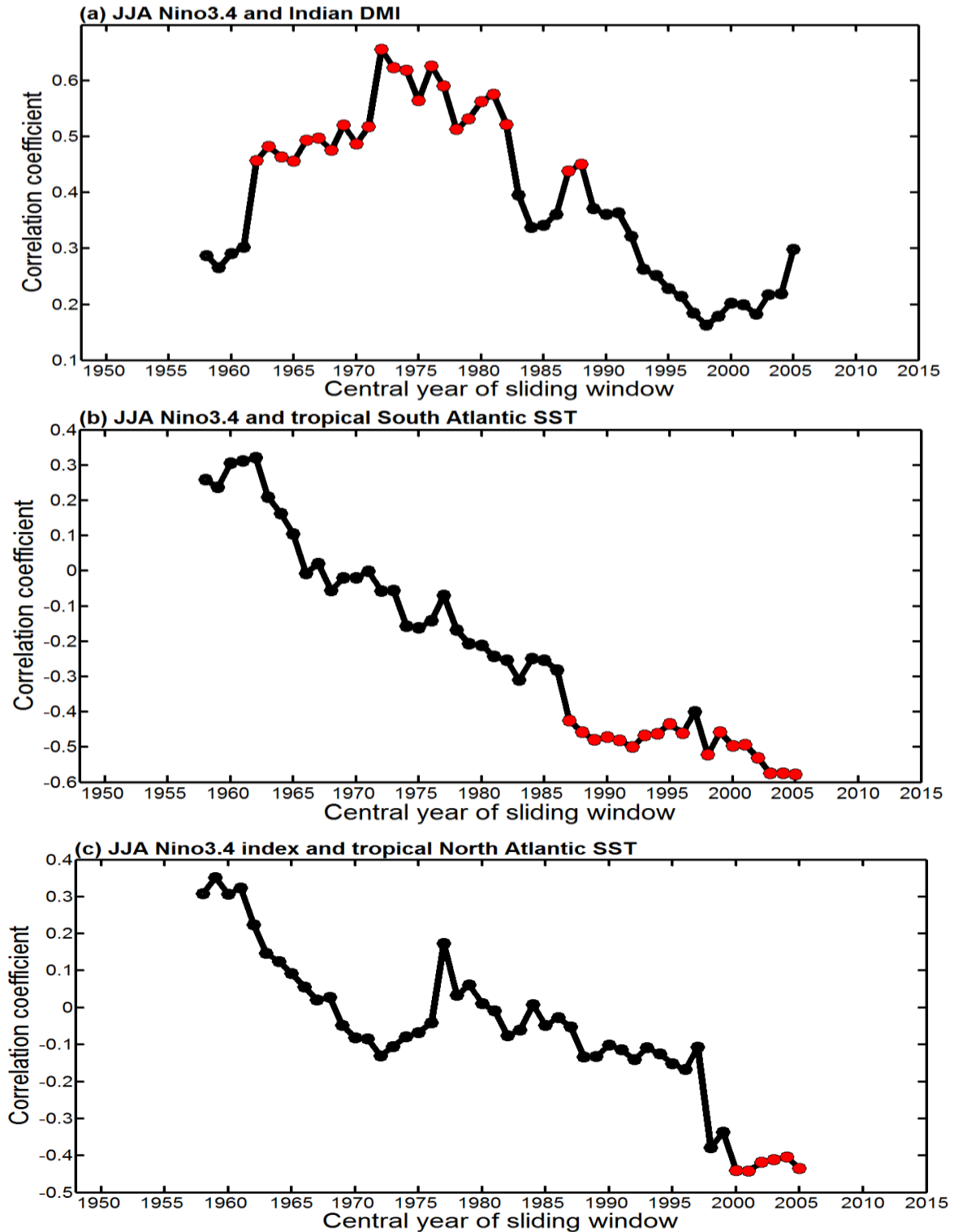


Figure 9. (a) The 21-year sliding correlation coefficients (e.g., the correlation coefficient in 2000 represents the period 1990–2010) between the JJA Niño3.4 and Indian DMI during 1948–2016. (b) Same as (a) but for the JJA Niño3.4 and tropical South Atlantic SSTs. According to *Kucharski et al.* (2008), the warm tropical South Atlantic SSTs could weaken the summer Indian monsoon. (c) Same as (a) but for the JJA Niño3.4 and tropical North Atlantic SSTs. According to *Hong et al.* (2014), the warm tropical North Atlantic SSTs could enhance the WNP subtropical high and weaken the summer WNP monsoon. The red dots represent correlations that are significant at the 95% confidence level.

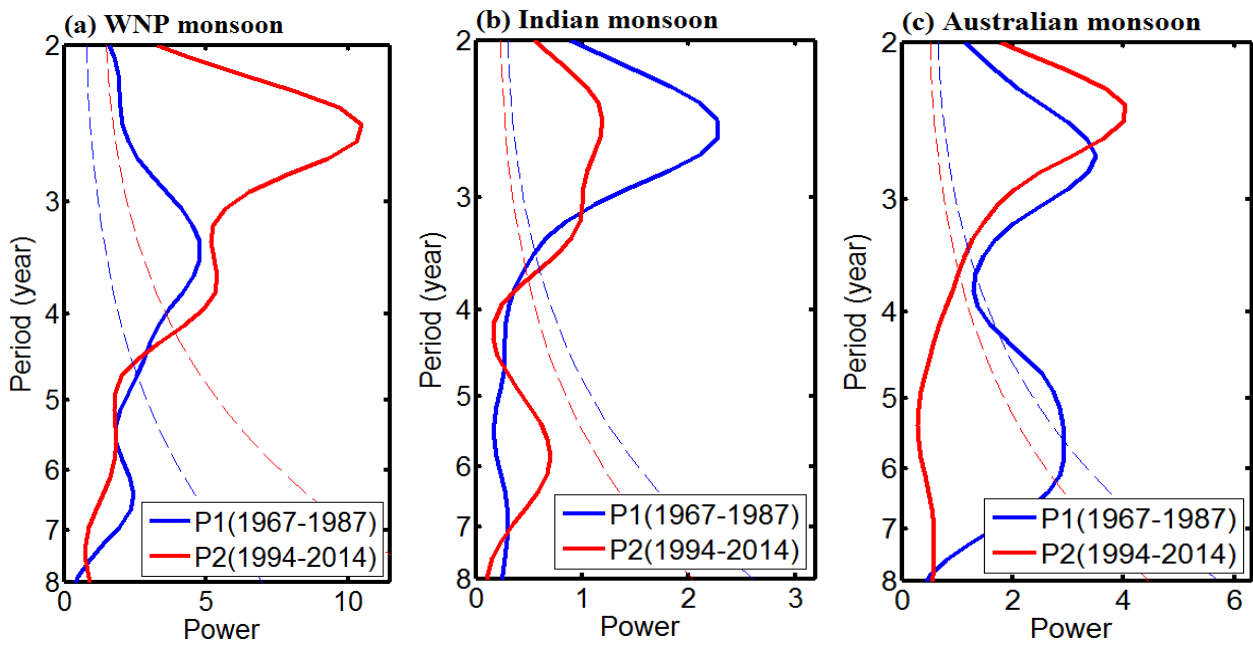
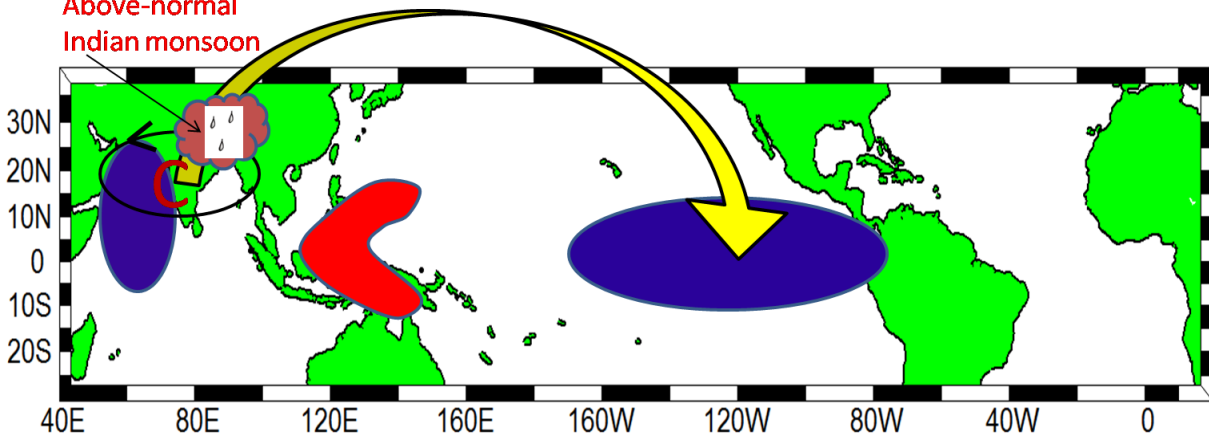


Figure 10. Comparison of power spectrum for the monsoon indices before and after the early 1990s. Distribution of power spectrum for (a) WNP monsoon, (b) Indian monsoon and (c) Australian monsoon. The dashed line denotes the 95% confidence interval against red noise.

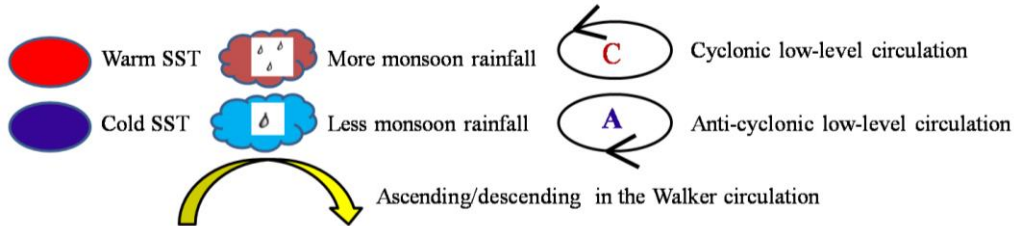
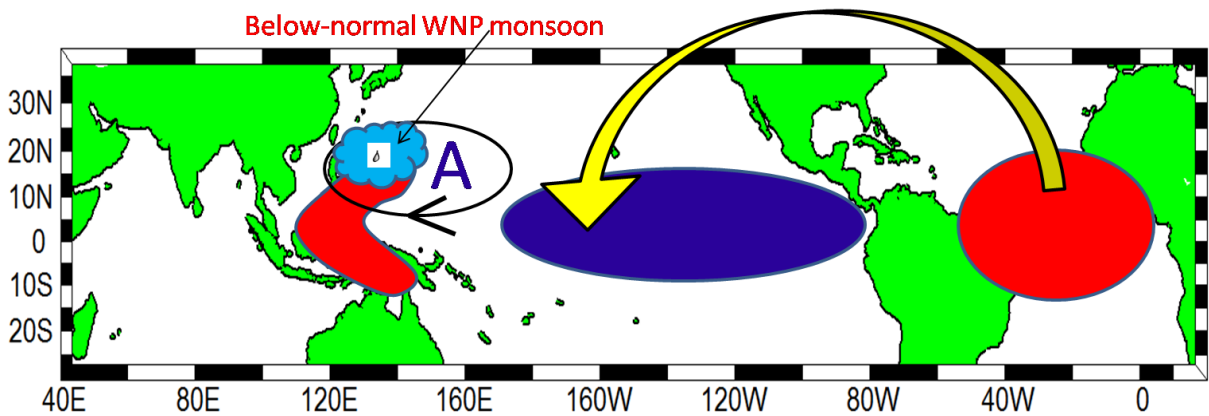
(a) Before the early-1990s: a stronger Pacific-Indian Ocean coherence/coupling

Above-normal
Indian monsoon



(b) After the early-1990s: a stronger Pacific-Atlantic coherence/coupling

Below-normal WNP monsoon



(c) Schematic summarizing the possible influences of the Atlantic Ocean on the TBO monsoon center

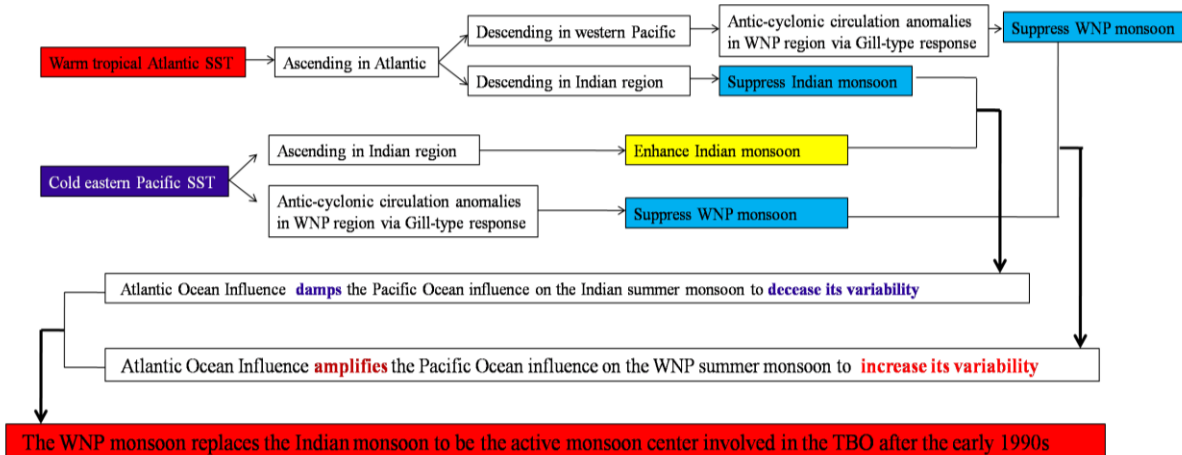


Figure 11. A schematic diagram showing the physical processes to induce the recent shift in the monsoon centers of the TBO. (a) The Pacific-Indian Ocean coherence/coupling before the early 1990s supports the Indian summer monsoon to be the monsoon center involved in the TBO. (b) The Pacific-Atlantic Ocean coherence/coupling after the early 1990s supports the WNP summer monsoon to be the monsoon center involved in the TBO. (c) The schematic summarizing the possible influences of the Atlantic Ocean on the shift of the summertime monsoon centers involved in the TBO.